Aerospace Science and Technology 15 (2011) 431–439

Contents lists available at ScienceDirect

Aerospace Science and Technology

www.elsevier.com/locate/aescte

Cascade-type guidance law design for multiple-UAV formation keeping

Tae Soo No [a,*,1], Youdan Kim [b,1], Min-Jea Tahk [c,1], Gyeong-Eon Jeon [a,2]

[a] Department of Aerospace Engineering, Chonbuk National University, Chonju, 560-756, Republic of Korea
[b] School of Mechanical and Aerospace Engineering, The Institute of Advanced Aerospace Technology, Seoul National University, Seoul 151-742, Republic of Korea
[c] Division of Aerospace Engineering, Korea Advanced Institute of Technology, Daejeon, 305-701, Republic of Korea

ARTICLE INFO

Article history:
Received 27 October 2008
Received in revised form 11 August 2010
Accepted 27 August 2010
Available online 1 September 2010

Keywords:
Formation flying
Unmanned aerial vehicle
Guidance and control
Lyapunov stability theorem
Nonlinear simulation

ABSTRACT

A procedure to compute guidance commands for controlling the relative geometry of multiple unmanned aerial vehicles (UAVs) in formation flight is proposed. The concepts of branch, global leader, and local leader/follower are used to represent the whole formation geometry. A positive-definite function defined in terms of the formation error is then introduced and the Lyapunov stability theorem is used to obtain the cascade type guidance law. This scheme leads to the synchronized flight of all UAVs while maintaining formation geometry. The results of a high fidelity nonlinear simulation of a reconnaissance and surveillance mission example are presented to show the effectiveness of the proposed guidance law.

1. Introduction

Flying a group of unmanned aerial vehicles (UAV) in formation has many applications in military missions such as reconnaissance and surveillance, target acquisition and designation, battle damage assessment, and the suppressions of enemy air defense as well as in civilian missions such as search and rescue, remote sensing, law enforcement, and communication relay service [7,9,16]. Although the results of successful flight tests of UAV formation flying have been reported [1,4,10,11], to fully operate such systems autonomously, in-depth research is still required in the areas of modeling, control, and guidance relevant to coordination and control problems [3,6,15,23]. In some cases, intelligence may be required for collision avoidance and formation reconfiguration but this depends greatly on the type of communication network and computational capability within the formation, and on the sensors equipped in each vehicle [2,22]. The technical issues that must be addressed for formation keeping range from single vehicle level issues to higher system level issues, the latter which define the system control hierarchy and the interface with human operators required for decision making and performance monitoring [12]. With respect to control and guidance problems in formation flying, each flight vehicle must be able to accept flight command from an outside source and carry out the assigned commands using its own flight control systems. The level of complexity and robustness of the overall formation depend on the communication and computation architecture among the distributed vehicles.

Formation keeping, in the context of this work, means that the relative positions between flight vehicles are tightly controlled so that the overall formation geometry remains unchanged. Several methods for formation keeping have been proposed [5,8,17–19,21,24]. In the prior literature, most of the control laws proposed for formation keeping have been based on the leader-follower framework. A leaderless coordination scheme was suggested in Ref. [17] to secure a formation robust to failures in one or more vehicles. The leader-follower formulation has advantages in that a control problem can be simplified as a standard tracking problem if the leader's information is available to the followers. In Refs. [5] and [24], a classical compensation type control law for formation keeping was presented. Treating formation keeping as a dynamic 3-D tracking problem, the classical compensation type control law decomposes the control task into three sub-tasks: vertical distance control, lateral distance control, and forward distance control. Guidance-based approaches have also been applied to the formation keeping problem. Naturally, the leader is treated as a target, and the follower is guided so that it maintains a required range from the leader instead of intercepting it [19,21]. This method requires no information flow from the leader to the follower vehicles. In Refs. [8,14,18], the aerodynamic coupling effects introduced by close formation flying were taken into account in the design of formation controllers.

The purpose of this work was to present a guidance law for the formation flight control of multiple UAVs. More specifically, we propose a method to generate the flight command inputs to UAV

* Corresponding author. Tel.: +82 63 270 2470.
E-mail address: rotthee@chonbuk.ac.kr (T.S. No).
[1] Professor.
[2] Graduate student.

1270-9638/$ – see front matter
doi:10.1016/j.ast.2010.08.011

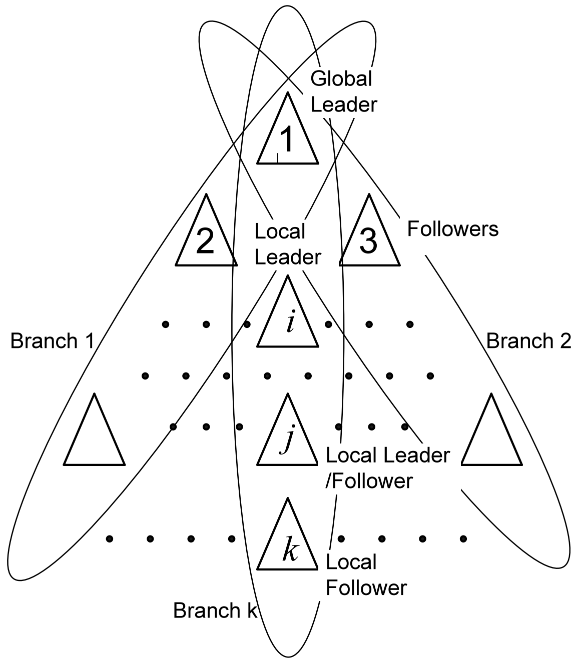

Fig. 1. Formation geometry.

k which will maintain the formation geometry as shown in Fig. 1. Herein, we introduce the concept of branch, global leader, local leader and local follower. Referring to Fig. 1, the whole formation is divided into several branches. Each branch is simply a chain of multiple UAVs that starts from the global leader UAV. Except for the global leader, other UAVs will take the role of a local leader, a local follower or both depending on their position in the branch. For the example formation geometry shown in Fig. 1, UAV j is not only the leader of UAV k but also the follower of UAV i. It should be noted that a particular UAV need not necessarily belong to only one specific branch but it may be a leader of several followers belonging to different branches. It will be assumed that one UAV can receive its local leader's flight information and also is able to transmit its own flight status to the local follower.

The organization of this paper is as follows: Section 2 describes the details for obtaining the guidance law. The results of high-fidelity nonlinear simulation studies are then presented in Section 3. Finally, Section 4 discusses the issues that require further consideration and finishes with brief conclusions.

2. Guidance law design

2.1. Model of UAV flight dynamics and control systems

The model for a UAV and its flight control systems was identical to that used in Ref. [13]. Referring to Stevens and Lewis [20], the equations of motion describing UAV flight dynamics are summarized as follows:

Force equations:

$$\begin{aligned}
\dot{U} &= RV - QW - g_0 \sin\theta + F_x/m \\
\dot{V} &= -RU + PW + g_0 \sin\phi \cos\theta + F_y/m \\
\dot{W} &= QU - PV + g_0 \cos\phi \cos\theta + F_z/m
\end{aligned} \tag{1}$$

Kinematic equations:

$$\begin{aligned}
\dot{\phi} &= P + \tan\theta(Q \sin\phi + R\cos\phi) \\
\dot{\theta} &= Q\cos\phi - R\sin\phi
\end{aligned}$$

Table 1
Definition of symbols used in the equations of motion.

Symbol	Definition
U, V, W	Components of translation velocity vector in the body-fixed frame
P, Q, R	Components of angular velocity (Roll, Pitch, Yaw)
ϕ, θ, ψ	Euler angles (Roll, Pitch, Yaw)
F_x, F_y, F_z	X, Y, and Z components of aerodynamics and thrust forces
L, M, N	Rolling, Pitching, and Yawing moments
p_N, p_E, h	Position components in the Earth-surface fixed frame (North, East, Altitude)
m	Mass of the aircraft
g_0	Gravity constant
c_i, $i = 1, 2, \ldots, 9$	Mass properties of the aircraft (see Stevens and Lewis, 1992)

$$\dot{\psi} = Q\sin\phi/\cos\theta + R\cos\phi/\cos\theta \tag{2}$$

Moment equations:

$$\begin{aligned}
\dot{P} &= (c_1 R + c_2 P)Q + c_3 L + c_4 N \\
\dot{Q} &= c_5 PR - c_6\left(P^2 - R^2\right) + c_3 M \\
\dot{R} &= (c_8 P - c_2 R)Q + c_4 L + c_9 N
\end{aligned} \tag{3}$$

Navigation equations:

$$\begin{aligned}
\dot{p}_N &= U\cos\theta\cos\psi + V(-\cos\phi\sin\psi + \sin\phi\sin\theta\cos\psi) \\
&\quad + W(\sin\phi\sin\psi + \cos\phi\sin\theta\cos\psi) \\
\dot{p}_E &= U\cos\theta\sin\psi + V(\cos\phi\cos\psi + \sin\phi\sin\theta\sin\psi) \\
&\quad + W(-\sin\phi\cos\psi + \cos\phi\sin\theta\sin\psi) \\
\dot{h} &= U\sin\theta - V\sin\phi\cos\theta - W\cos\phi\cos\theta
\end{aligned} \tag{4}$$

The fact that the aerodynamic and propulsive forces and moments are complex functions of flight conditions and deflection of control surfaces was fully accounted for. A first-order system was adopted to model the control surface servos, and the maximum deflection of the control surfaces was limited to $\pm 30°$. The engine dynamics and throttle opening were similarly modeled as a first-order system. Readers are referred to Table 1 and Ref. [20] for the definitions of the symbols used in Eqs. (1)–(4), and the mass and physical properties of the flight vehicle.

The linearized equations of motion and standard classical method such as root-locus and frequency response analysis were used to build the flight control systems. As can be seen in Fig. 2, PID (proportional-integral-derivative) and lead/lag type controllers were extensively used to model various, internal controllers for stability and control augmentation. Finally, the three outer-most channels for the speed (v), flight path angle (γ), and heading angle (ψ) controls completed the flight control systems.

As the explicit mathematical expression of the flight dynamics and control systems represented by Eqs. (1)–(4) and Fig. 2 is practically impossible, we reduced this complex model to a simpler model for the restricted purpose of guidance law design. Accordingly, we adopted first-order systems to represent three control channels including the UAV flight dynamics as follows:

$$\dot{v} = \frac{1}{\tau_v}(v_c - v) \quad \text{(speed control channel)} \tag{5}$$

$$\dot{\psi} = \frac{1}{\tau_\psi}(\psi_c - \psi) \quad \text{(heading angle control channel)} \tag{6}$$

$$\dot{\gamma} = \frac{1}{\tau_\gamma}(\gamma_c - \gamma) \quad \text{(flight path angle control channel)} \tag{7}$$

where (v_c, ψ_c, γ_c) and $(\tau_v, \tau_\psi, \tau_\gamma)$ denote, respectively, the time constant of and the control command input to each control loop.

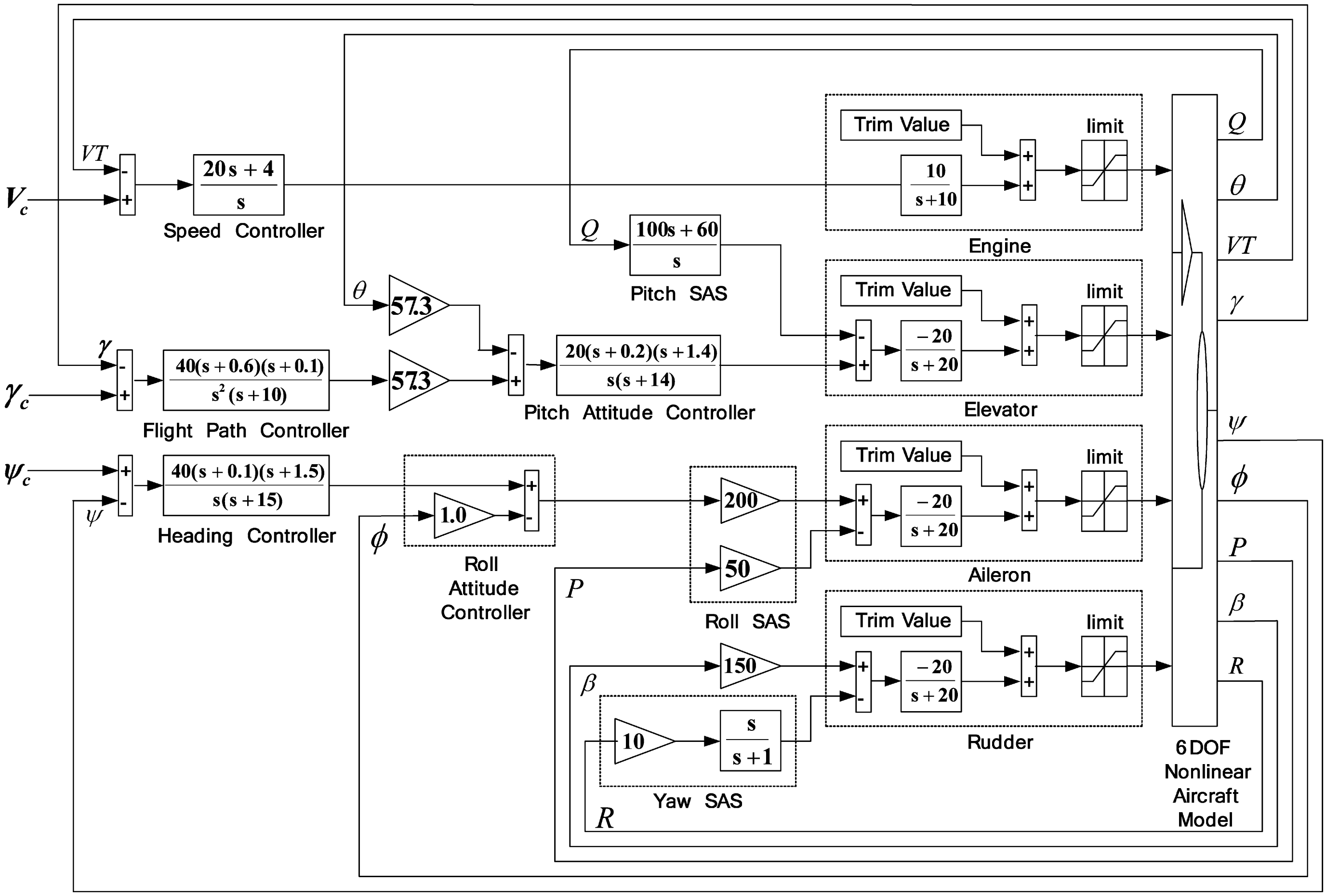

Fig. 2. UAV dynamics and control system.

To determine the time constant, the time histories of the flight speed and directional responses to a given set of (or individual) commands in the nonlinear model were generated using the nonlinear simulation, and these outputs were then curve-fitted to the first-order model.

2.2. Guidance law design

Referring to Fig. 3, $\boldsymbol{d}^i$ and $\boldsymbol{v}^i$ denote the current position of UAV i and its velocity vectors, respectively. If two UAVs j and k maintain their current flight directions and speeds, then their relative position vector at a later t_{go} can be written as:

$$\Delta\boldsymbol{d} = (\boldsymbol{d}^j - \boldsymbol{d}^k) + (\boldsymbol{v}^j - \boldsymbol{v}^k)t_{go} \tag{8}$$

If neither of these UAVs takes corrective measures, the expected formation error at a future time $t + t_{go}$ will be

$$\delta\boldsymbol{d} = \Delta\boldsymbol{d} - \Delta\boldsymbol{d}^*$$

where $\Delta\boldsymbol{d}^*$ is the required relative position vector between UAV j and k for formation flying.

Referring to Fig. 4 and using $(\boldsymbol{e}_x, \boldsymbol{e}_y, \boldsymbol{e}_z)$ to denote the unit vectors of the fixed inertial frame, we can write the formation error, the absolute velocity and the acceleration vectors of a UAV in terms of its speed and flight direction angles (heading and flight path), respectively, as

$$\delta\boldsymbol{d} = M_x\boldsymbol{e}_x + M_y\boldsymbol{e}_y + M_z\boldsymbol{e}_z \tag{9}$$

$$\begin{aligned}\boldsymbol{v} &= v_x\boldsymbol{e}_x + v_y\boldsymbol{e}_y + v_z\boldsymbol{e}_z \\ &= (v\cos\gamma\cos\psi)\boldsymbol{e}_x + (v\cos\gamma\sin\psi)\boldsymbol{e}_y - (v\sin\gamma)\boldsymbol{e}_z\end{aligned} \tag{10}$$

$$\begin{aligned}\frac{d\boldsymbol{v}}{dt} &= (\dot{v}\cos\gamma\cos\psi - v\dot{\gamma}\sin\gamma\cos\psi - v\dot{\psi}\cos\gamma\sin\psi)\boldsymbol{e}_x \\ &\quad + (\dot{v}\cos\gamma\sin\psi - v\dot{\gamma}\sin\gamma\sin\psi + v\dot{\psi}\cos\gamma\cos\psi)\boldsymbol{e}_y \\ &\quad - (\dot{v}\sin\gamma + v\dot{\gamma}\cos\gamma)\boldsymbol{e}_z\end{aligned} \tag{11}$$

We now introduce a UAV control frame, $(\boldsymbol{e}_v, \boldsymbol{e}_\psi, \boldsymbol{e}_\gamma)$, where $\boldsymbol{e}_v$ denotes a unit direction vector along the current velocity vector, $\boldsymbol{e}_\psi$ is a unit direction vector perpendicular to $\boldsymbol{e}_v$ and positive in the sense of increasing heading angle, and $\boldsymbol{e}_\gamma$ completes the right-handed system. Then, the coordinate transformation matrix $\boldsymbol{D}$ from the fixed inertial frame to the UAV control frame can be defined as

$$\boldsymbol{D} = \begin{bmatrix} \cos\psi\cos\gamma & \sin\psi\cos\gamma & -\sin\gamma \\ -\sin\psi & \cos\psi & 0 \\ \cos\psi\sin\gamma & \sin\psi\sin\gamma & \cos\gamma \end{bmatrix} \tag{12}$$

Rewriting Eqs. (9)–(11) in the UAV control frame using the transformation matrix $\boldsymbol{D}$ yields

$$\delta\boldsymbol{d} = M_v\boldsymbol{e}_v + M_\psi\boldsymbol{e}_\psi + M_\gamma\boldsymbol{e}_\gamma \tag{13}$$

$$\boldsymbol{v} = v\boldsymbol{e}_v \tag{14}$$

$$\frac{d\boldsymbol{v}}{dt} = \dot{v}\boldsymbol{e}_v + v\dot{\psi}\cos\gamma\boldsymbol{e}_\psi - v\dot{\gamma}\boldsymbol{e}_\gamma \tag{15}$$

where $(M_v, M_\psi, M_\gamma)^T = \boldsymbol{D}(M_x, M_y, M_z)^T$.

Assuming that the differences in the flight path and heading angles of both the leader UAV j and follower UAV k are small,

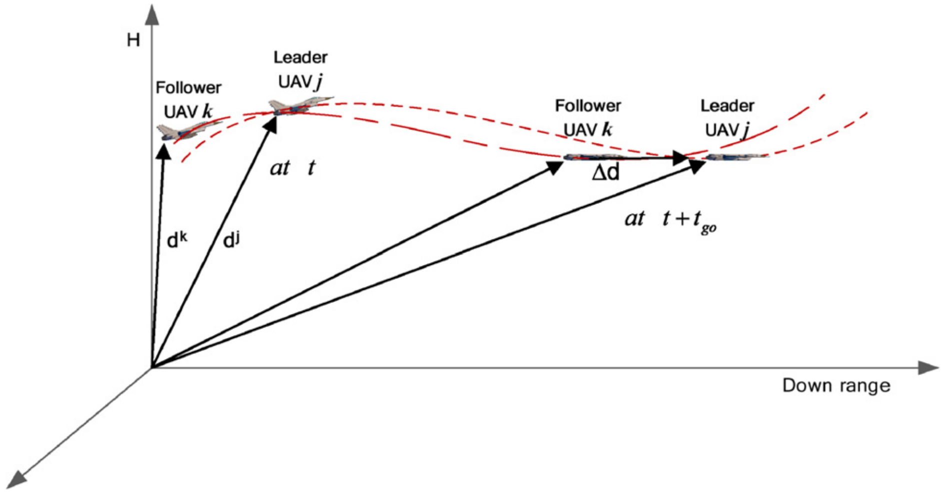

Fig. 3. Leader-follower geometry.

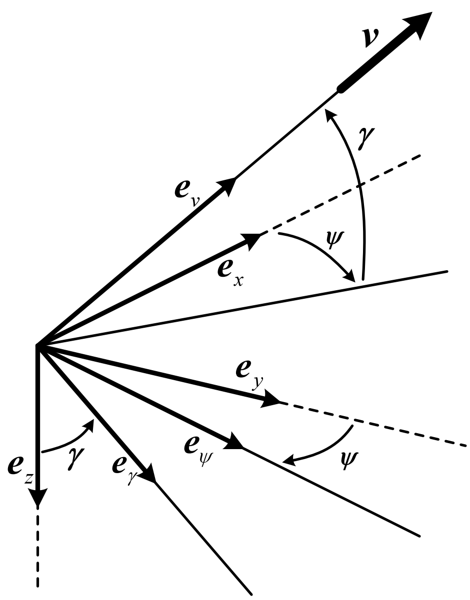

Fig. 4. UAV control frame.

we can define another coordinate transformation matrix from the follower UAV k's control frame to the leader UAV j's frame as:

$$\delta\boldsymbol{D} = \begin{bmatrix} 1 & \delta\psi & -\delta\gamma \\ -\delta\psi & 1 & 0 \\ \delta\gamma & 0 & 1 \end{bmatrix} \tag{16}$$

where $\delta\gamma = \gamma^j - \gamma^k$ is the flight path angle difference, and $\delta\psi = \psi^j - \psi^k$ is the yaw angle difference. Hereinafter, a superscript i is used to denote a quantity that is related to UAV i or expressed in its control frame. Using this notation, we can express the velocity vector of the leader UAV, $\boldsymbol{v}^j$ in the follower UAV k's control frame $(\boldsymbol{e}_v^k, \boldsymbol{e}_\psi^k, \boldsymbol{e}_\gamma^k)$ as:

$$\boldsymbol{v}^j = v^j\boldsymbol{e}_v^k + v^j\delta\psi\boldsymbol{e}_\psi^k - v^j\delta\gamma\boldsymbol{e}_\gamma^k \tag{17}$$

Similarly, the acceleration vector of the leader UAV j in the follower UAV k's control frame can be written as

$$\begin{aligned}\frac{d\boldsymbol{v}^j}{dt} &= \left(\dot{v}^j - \dot{\psi}^j v^j\delta\psi\cos\gamma^j - \dot{\gamma}^j\delta\gamma v^j\right)\boldsymbol{e}_v^k \\ &\quad + \left(\dot{v}^j\delta\psi + \dot{\psi}^j v^j\cos\gamma^j\right)\boldsymbol{e}_\psi^k + \left(-\dot{v}^j\delta\gamma - \dot{\gamma}^j v^j\right)\boldsymbol{e}_\gamma^k \end{aligned} \tag{18}$$

Next, we define a positive definite function:

$$\begin{aligned} L &= \frac{1}{2}\delta\boldsymbol{d}\cdot\delta\boldsymbol{d} \\ &= \frac{1}{2}(\Delta\boldsymbol{d} - \Delta\boldsymbol{d}^*)\cdot(\Delta\boldsymbol{d} - \Delta\boldsymbol{d}^*) \end{aligned} \tag{19}$$

If the follower UAV k is controlled so that the value of Eq. (19) remains small for a sufficiently short time t_{go}, then $\Delta\boldsymbol{d}$ will remain close to $\Delta\boldsymbol{d}^*$, and this implies that their relative positions are maintained. To determine this, differentiating Eq. (19) and writing it in the follower UAV k's control frame gives:

$$\begin{aligned} \frac{dL}{dt} &= \left(\frac{d\boldsymbol{v}^j}{dt} - \frac{d\boldsymbol{v}^k}{dt}\right)\cdot(\Delta\boldsymbol{d} - \Delta\boldsymbol{d}^*)t_{go} \\ &= \left(\dot{v}^j - \dot{\psi}^j v^j\delta\psi\cos\gamma^j - \dot{\gamma}^j\delta\gamma v^j - \dot{v}^k\right)M_v^k t_{go} \\ &\quad + \left(\dot{v}^j\delta\psi + \dot{\psi}^j v^j\cos\gamma^j - v^k\dot{\psi}^k\cos\gamma^k\right)M_\psi^k t_{go} \\ &\quad + \left(-\dot{v}^j\delta\gamma - \dot{\gamma}^j v^j + \dot{\gamma}^k v^k\right)M_\gamma^k t_{go} \end{aligned} \tag{20}$$

where it is assumed that the required geometry $\Delta\boldsymbol{d}^*$ is constant, and $(M_v^k, M_\psi^k, M_\gamma^k)$ are the components of $(\Delta\boldsymbol{d} - \Delta\boldsymbol{d}^*)$ written in the follower UAV k's control frame.

Among many alternatives to make Eq. (20) negative definite, we chose to use the following:

$$\begin{aligned} \frac{dL}{dt} &= -2N^k L \\ &= -N^k\left(M_v^k\right)^2 - N^k\left(M_\psi^k\right)^2 - N^k\left(M_\gamma^k\right)^2 \end{aligned} \tag{21}$$

where N^k is a positive constant and the fact that $L = \frac{1}{2}((M_v^k)^2 + (M_\psi^k)^2 + (M_\gamma^k)^2)$ is used. Keeping in mind that the purpose here is to find the guidance commands for the UAV k, direct comparison of Eqs. (20) and (21) yields:

$$\begin{aligned} \dot{v}^k &= \left(\dot{v}^j - \dot{\psi}^j v^j\delta\psi\cos\gamma^j - \dot{\gamma}^j\delta\gamma v^j\right) + \frac{N^k}{t_{go}}M_v^k \\ \dot{\psi}^k &= \frac{(\dot{v}^j\delta\psi + \dot{\psi}^j v^j\cos\gamma^j)}{v^k\cos\gamma^k} + \frac{N^k}{t_{go}}\frac{1}{v^k\cos\gamma^k}M_\psi^k \\ \dot{\gamma}^k &= \frac{(\dot{v}^j\delta\gamma + \dot{\gamma}^j v^j)}{v^k} - \frac{N^k}{t_{go}}\frac{1}{v^k}M_\gamma^k \end{aligned} \tag{22}$$

which are the required rates of change in the speed and flight direction angles of UAV k to decrease the formation error. Now the problem becomes how UAV k should be controlled to follow the reference model described by Eq. (22). Because a simple, first-order

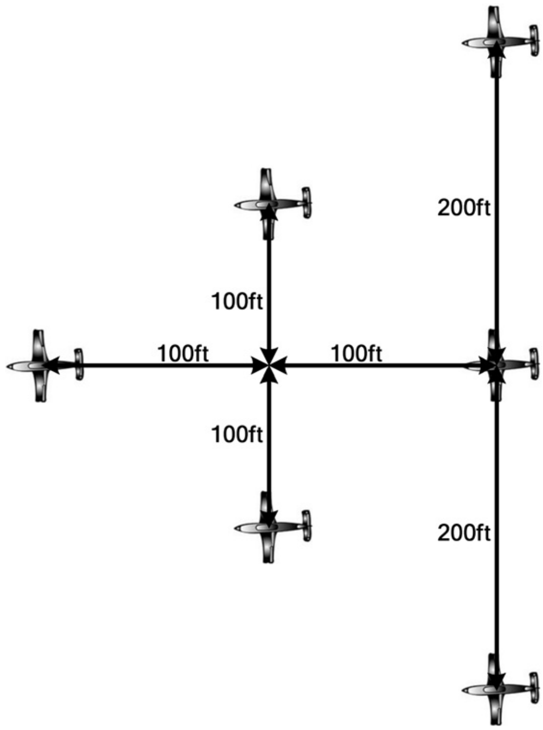

Fig. 5. Six (6) UAVs in formation flight.

model, as in Eqs. (5)–(7), was adopted, we can compare Eqs. (5)–(7) and Eq. (22) to find the guidance commands, $(v_c^k, \psi_c^k, \gamma_c^k)$ for UAV k as follows:

$$v_c^k = \left[v^k + \tau_v^k\left(\dot{v}^j - \dot{\psi}^j v^j \delta\psi \cos\gamma^j - \dot{\gamma}^j \delta\gamma v^j\right)\right] + \left[N^k \frac{\tau_v^k}{t_{go}} M_v^k\right]$$
$$\psi_c^k = \left[\psi^k + \frac{\tau_\psi^k(\dot{v}^j \delta\psi + \dot{\psi}^j v^j \cos\gamma^j)}{v^k \cos\gamma^k}\right] + \left[N^k \frac{\tau_\psi^k}{t_{go}} \frac{1}{v^k \cos\gamma^k} M_\psi^k\right]$$
$$\gamma_c^k = \left[\gamma^k + \frac{\tau_\gamma^k(\dot{v}^j \delta\gamma + \dot{\gamma}^j v^j)}{v^k}\right] - \left[N^k \frac{\tau_\gamma^k}{t_{go}} \frac{1}{v^k} M_\gamma^k\right] \tag{23}$$

From the above equations, we find that the guidance commands for the follower UAV k may be computed using any available information such as its own and the leader UAV j's flight conditions, control system characteristics, and the formation keeping error, $(M_v^k, M_\psi^k, M_\gamma^k)$. These guidance commands are composed of two parts. The first part accounts for differences in the flight speed and directions between the leader and the follower UAVs at the current time, and the second part generates additional commands that are proportional to the formation error. The navigation gains N^k and t_{go} play the role of proportionality constants. These parameters should be chosen considering factors such as the controller bandwidth and the actuator limit although any positive values will work for the linear systems.

Fig. 6. Flight trajectory for reconnaissance and surveillance mission (plan view).

The acceleration information of the leader UAV j is also required through $(\dot{v}^j, \dot{\psi}^j, \dot{\gamma}^j)$. However, the flight conditions (v^j, ψ^j, γ^j) and flight commands $(v_c^j, \psi_c^j, \gamma_c^j)$ can be substituted by the acceleration information if the leader UAV j's dynamics can be approximated by a first-order system similarly to the follower UAV k. This means that the flight status of and commands for the leader UAV must be communicated to the follower UAV. The same procedure can be applied to another pair of leader and follower UAVs that belong to the same branch. Eventually, all the UAVs in the formation are connected in a cascade, allowing one UAV to access the flight information of all its leader UAVs.

3. Numerical simulation example

The example scenario used in the simulation is a reconnaissance and surveillance mission where the UAV fleet is required to fly over a pre-designated area. Referring to Fig. 5, the fleet is composed of six UAVs: the global leader UAV will track the pre-uploaded flight commands in Table 2, which are designed to cover the pre-designated area shown in Fig. 6. Other follower UAVs should form a triangular formation. The position of each UAV relative to the positions of its neighboring UAVs is described in Fig. 5. It is assumed that all six UAVs are initially flying at the speed of 350 ft/s and at the altitude of 1500 ft.

There are many possibilities in the formation structure. Fig. 7 shows two example formations where the number of branches is three and four. One can easily see that the roles of a UAV vary depending on the formation structure. The role of UAV 5 in Fig. 7(a), for example, is as the follower of the formation global leader and it does not have any followers. However, in the four-branch-formation shown in Fig. 7(b), it is not only the follower of the global leader but also is the leader of two followers. Fig. 8 shows an internal view of each UAV block in Fig. 7. The "Command Shaping" block computes the guidance commands using its own and the leader UAV's flight information. These commands are used as a set of reference inputs to the flight control system in the

Table 2
Flight command schedule for reconnaissance and surveillance mission (applied to the global leader only).

Way point	Mission	Time (sec)	Speed (ft/s)	Fight path angle	Heading angle
Wp. 1	Target acquisition	50 $(=t_1)$	$V_c = 350$	$\gamma_C = 0°$	$\psi_c = 0°$
Wp. 2	Ingress	350 $(=t_2)$	$V_c = 350 - \frac{1}{3}(t - t_1)$	$\gamma_C = 0.995°$	$\psi_c = 0°$
Wp. 3	Mission	615 $(=t_3)$	$V_c = 250$	$\gamma_C = 0°$	$\psi_c = \frac{495°}{265}(t - t_2)$
Wp. 4	Ingress	915 $(=t_4)$	$V_c = 250 + \frac{1}{6}(t - t_3)$	$\gamma_C = -0.5209°$	$\psi_c = 495°$
Wp. 5	Mission	1235 $(=t_5)$	$V_c = 300$	$\gamma_C = 0°$	$\psi_c = 495° + \frac{450°}{320}(t - t_4)$
Wp. 6	Digress	1350 $(=t_6)$	$V_c = 300$	$\gamma_C = 0°$	$\psi_c = 945°$
Wp. 7	Return	1600	$V_c = 300 - \frac{1}{5}(t - t_6)$	$\gamma_C = -0.625°$	$\psi_c = 945°$

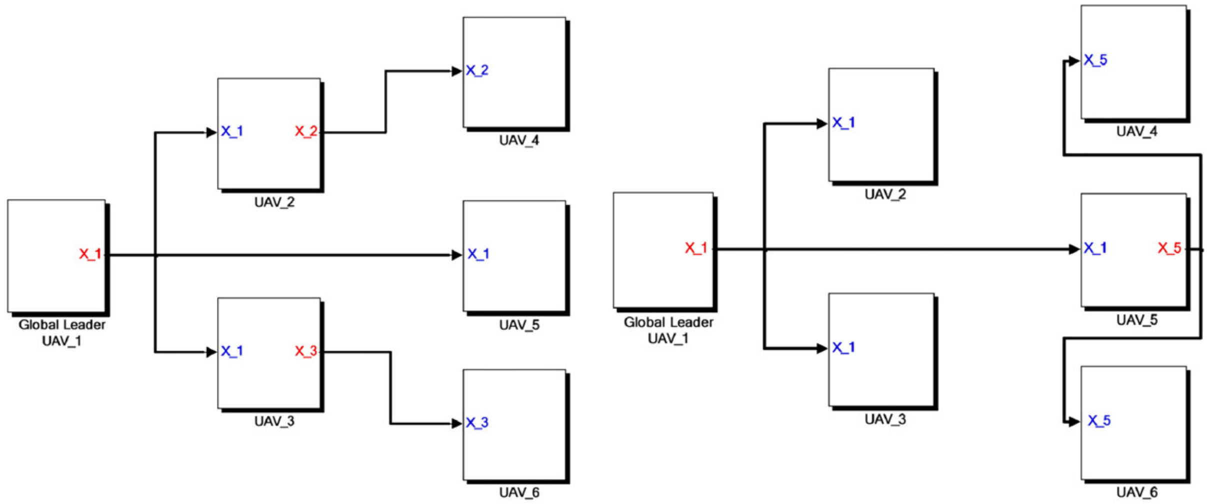

(a) Three branches (b) Four branches

Fig. 7. Different formation architectures.

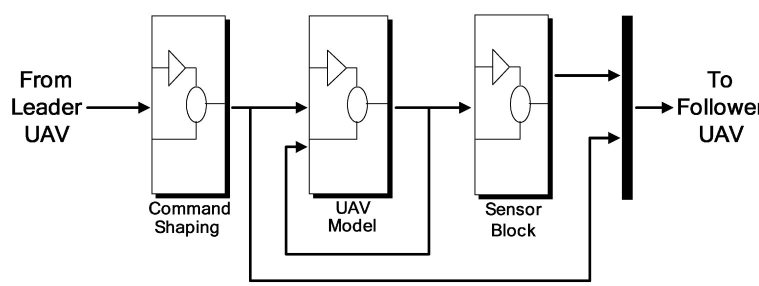

Fig. 8. Internal control structure of a UAV.

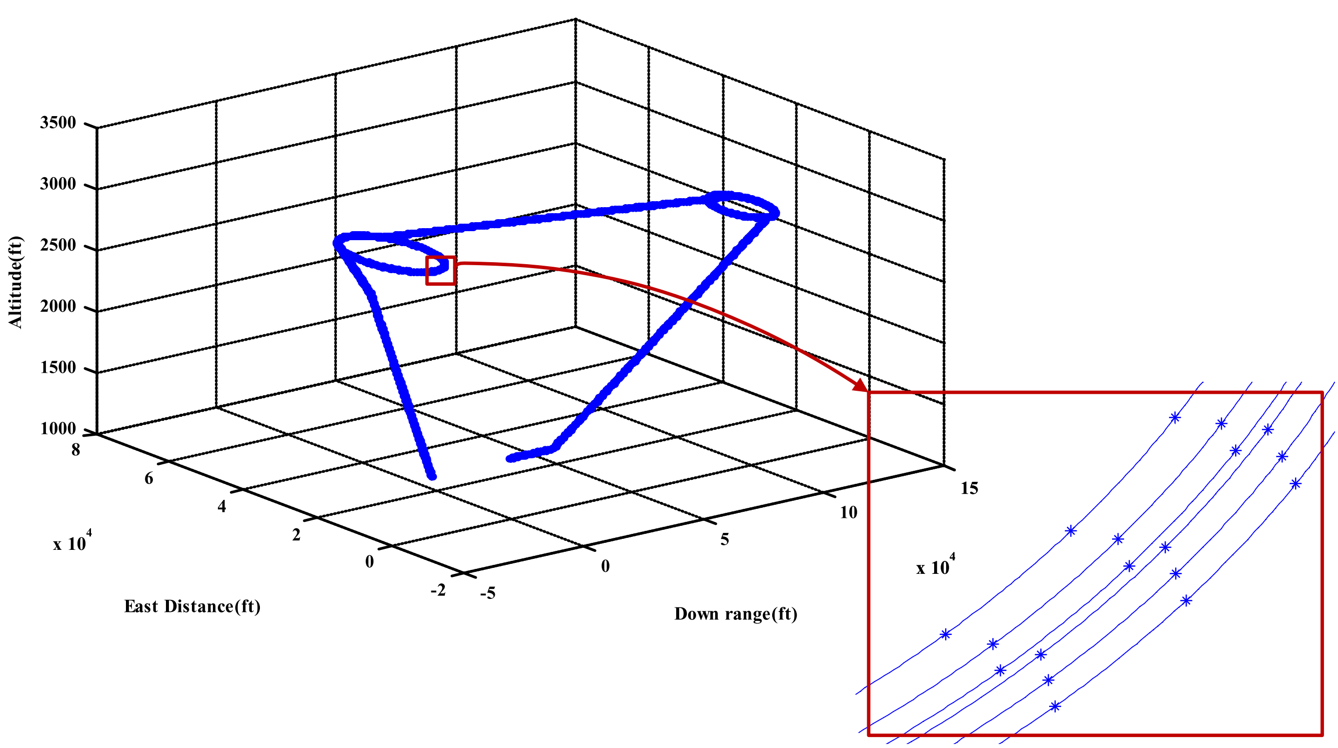

Fig. 9. Achieved flight trajectories.

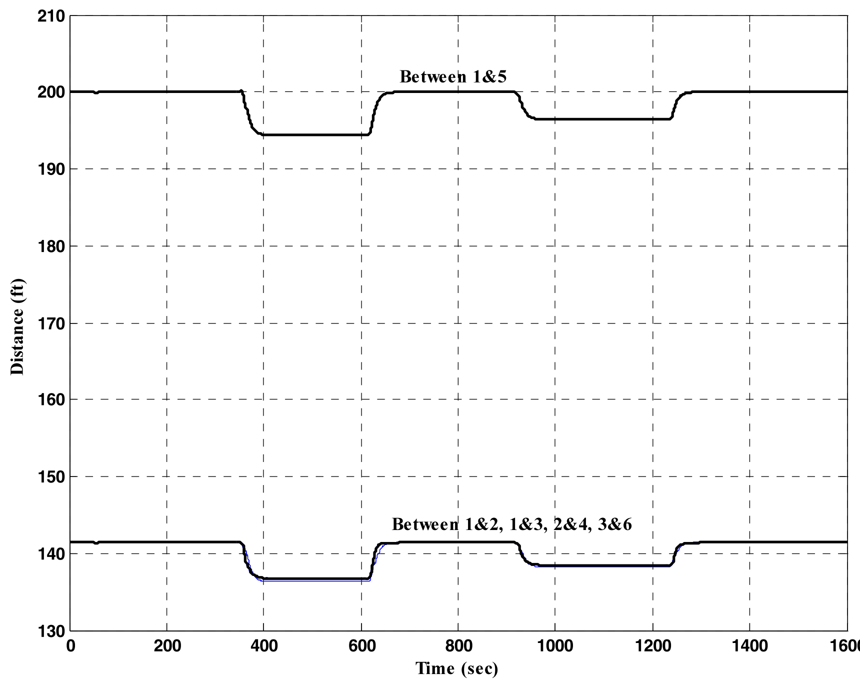

Fig. 10. Distance differences between UAVs.

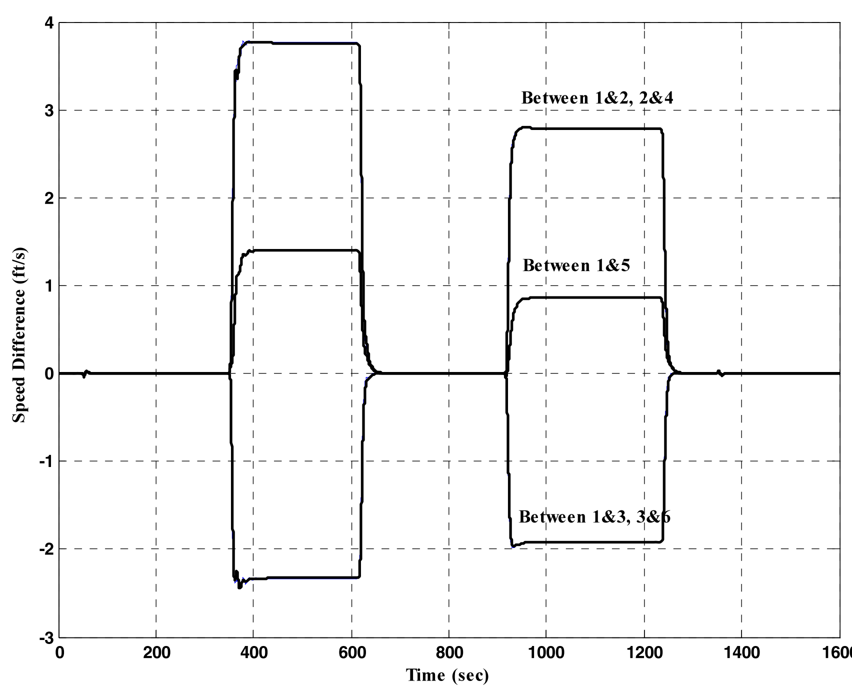

Fig. 11. Speed differences between UAVs.

"UAV Model" block: this is identical to the nonlinear UAV model shown in Fig. 2. Finally, the guidance commands and other flight information are passed down to the next follower UAV. It should be noted that any communication delay or sensor noise is not considered in the present work.

In this simulation example, it is assumed that all UAVs have the same aerodynamic and physical characteristics. Readers are referred to Ref. [13] for more details. As the results from both three-branch and four-branch formation architecture were almost identical, only those of the three-branch formation are discussed in the following. The guidance gains N^k and t_{go} used in the numerical example were, respectively, 1 and 8.

In Figs. 9 and 10, respectively showing the three-dimensional trajectory and the distance between UAVs, it is apparent that the six UAVs maintained the required formation geometry during their flight. The global leader UAV flew according to the flight schedule defined in Table 2 and the remaining UAVs controlled their positions in the formation using the guidance commands described in Section 2. Figs. 11 and 12 show that the differences in the flight speed and heading between the leader and the follower

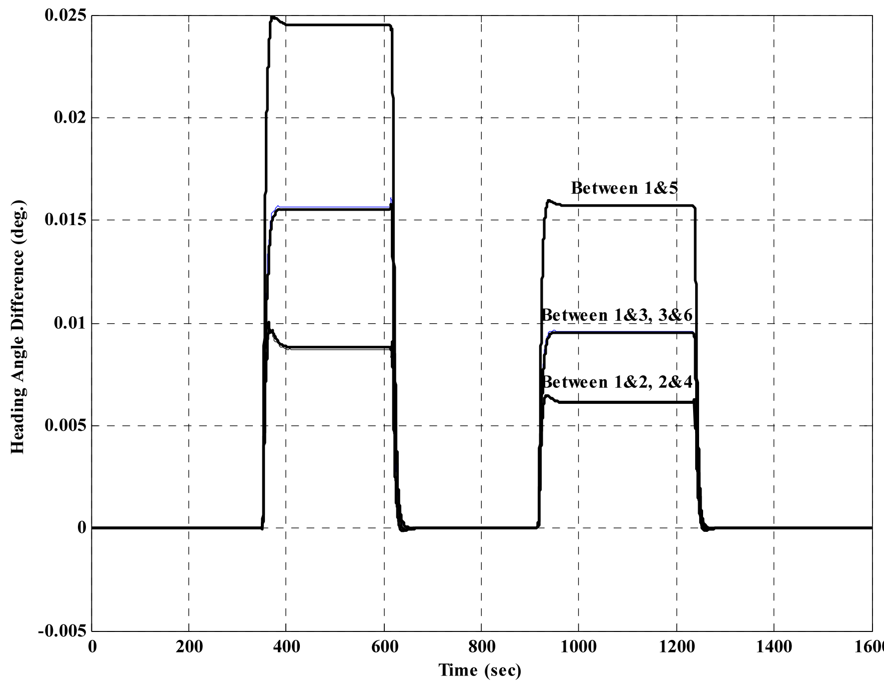

Fig. 12. Heading angle differences between UAVs.

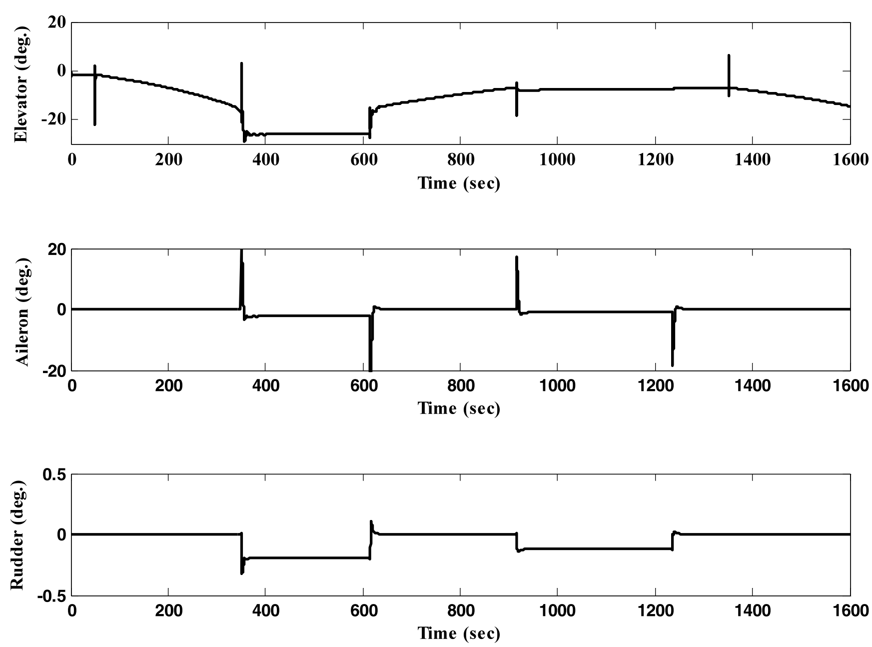

Fig. 13. Time histories of control surface deflections.

UAVs were very small throughout the flight. Although not shown here, the difference in the flight path angle was almost negligible. These small differences imply that all UAVs perform a synchronized flight. However, there was an almost constant difference in speed during the time when a turning flight was required because a UAV should fly faster or slower than the global leader UAV depending on its location relative to the global leader. Finally, the movements of three control surfaces (elevator, aileron, and rudder) are shown in Fig. 13. The elevator moved in response to the flight speed change. The aileron and the rudder deflection angles remain at zero during the flight in the vertical plane, but they automatically sought the steady-state values required for the coordinated turning phase.

4. Conclusions and comments on future work

In this study, a guidance scheme for the formation flying of multiple UAVs was proposed, and the results from fully nonlinear six degrees of freedom simulations were presented to show the effectiveness of this scheme for formation keeping. The entire formation was assumed to be composed of a number of branches with a chain of several UAVs forming a branch. In each branch, a pair of UAVs took either the roles of local leader or follower. The follower UAV calculated the control commands by using not only its own flight status and formation error information but also the leader's flight status and commands. In this manner, each UAV had full access to the flight information of all its leader UAVs and this result in a cascade type guidance law for formation keeping. A simulation study was carried out using a fleet of six UAVs for an example reconnaissance and surveillance mission. The formation leader performed a preprogrammed maneuver and the other remaining vehicles were required to fly cooperatively to maintain the required formation geometry. The simulation results showed that the formation was tightly controlled and all the UAVs performed an almost synchronized flight.

As performance of not only the present method but also other guidance scheme will greatly rely on the communication network between UAVs, issues such as communication delay, speed and amount of data traffic, sensor noise, etc., warrant in-depth investigations for actual implementation. It should be also noted that in this kind of close-formation flying, there exists the chance of collision between UAVs during formation keeping maneuvers due to unexpected external disturbances and/or the malfunctioning of a UAV. These problems are better considered at higher levels of the system control architecture and operational concept.

Acknowledgements

The authors gratefully acknowledge the financial support of the Agency for Defense Development and the FVRC (Flight Vehicle Research Center), Seoul National University.

References

[1] S. Bayraktar, G.E. Fainekos, G.J. Pappas, Experimental cooperative control of fixed-wing unmanned aerial vehicles, in: Proceedings of the 43rd IEEE Conference on Decision and Control, Atlantis, Paradise Island, Bahamas, December 2004.

[2] S. Bayraktar, G.E. Fainekos, G.J. Pappas, Hybrid modeling and experimental cooperative control of multiple unmanned aerial vehicles, Technical Report MS-CIS-04-32, Department of Computer and Information Science, University of Pennsylvania, December 2004.

[3] D.G. Bowen, S.C. MacKenzie, Autonomous collaborative unmanned vehicles: technological drivers and constraints, Defence R&D Canada, Contract Report DRDC CR-2003-003, September 2003.

[4] G. Campa, M.R. Napolitano, B. Seanor, M.G. Perhinschi, Design of control laws for maneuvered formation flight, in: Proceedings of the 2004 American Control Conference, Boston, Massachusetts, June–July 2004.

[5] G. Campa, B. Seanor, Y. Gu, M.R. Napolitano, NLDI guidance laws for close formation flight, in: 2005 American Control Conference, Portland OR, June 2005.

[6] P.R. Chandler, M. Pachter, D. Swaroop, J.M. Fowler, J.H. Howlett, S. Rasmussen, C. Schumacher, K. Nygard, Complexity in UAV cooperative control, in: Proceedings of the American Control Conference, Anchorage, AK, May 2002.

[7] Development and Operation of UAVs for Military and Civil Applications, North Atlantic Treaty Organization, RTO Education Notes 9, April 2000.

[8] A. Dogan, S. Venkataramanan, Nonlinear control for reconfiguration of unmanned-aerial-vehicle formation, Journal of Guidance, Control, and Dynamics 28 (4) (July–August 2005).

[9] M. Flint, M. Polycarpou, E. Fernandez-Gaucherand, Cooperative control for multiple autonomous UAV's searching for targets, in: Proceedings of the 41st IEEE Conference on Decision and Control, Las Vegas, Nevada, December 2002.

[10] J. How, E. King, Y. Kuwata, Flight demonstrations of cooperative control for UAV teams, in: AIAA 3rd "Unmanned Unlimited" Technical Conference, Workshop and Exhibit, Chicago, Illinois, September 2004.

[11] E. King, Y. Kuwata, L. Bertuccelli, J. How, Coordination and control experiments on multi-vehicle testbed, in: Proceedings of the 2004 American Control Conference, Boston, Massachusetts, June–July 2004.

[12] P. Narayan, P. Wu, D. Campbell, R. Walker, An intelligent control architecture for unmanned aerial systems (UAV) in the national airspace system (NAS), in: 2nd Australian Unmanned Air Vehicle Systems Conference, March 2007.

[13] T.S. No, B.M. Min, R.H. Stone, K.C. Wang, Control and simulation of arbitrary flight trajectory-tracking, Control Engineering Practice 13 (2005) 601–612.

[14] M. Pachter, J.J. D'Azzo, A.W. Proud, Tight formation flight control, Journal of Guidance, Control, and Dynamics 24 (2) (March–April 2001).

[15] C.A. Rabbath, E. Gagnon, M. Lauzon, On the cooperative control of multiple unmanned aerial vehicles, IEEE Canadian Review (Spring 2004) 15–19.

[16] Z. Sarris, Survey of UAV applications in civil markets, available on-line at http://med.ee.nd.edu/MED9/Papers/Aerial_vehicles/med01-164.pdf, June 2001.

[17] R. Sattigeri, A.J. Calise, An adaptive vision-based approach to decentralized formation control, AIAA 2004-5252, in: AIAA Guidance, Navigation, and Control Conference and Exhibit, Providence, Rhode Island, August 2004.

[18] C.J. Schumacher, R. Kumar, Adaptive control of UAVs in close-coupled formation flight, in: Proceedings of the American Control Conference, Chicago, Illinois, June 2000.

[19] S. Segal, J.Z. Ben-Asher, H. Weiss, Derivation of formation-flight guidance laws for unmanned air vehicles, Journal of Guidance, Control, and Dynamics 28 (4) (July–August 2005).

[20] B.L. Stevens, F.L. Lewis, Aircraft Control and Simulation, John Wiley & Sons, Inc., USA.

[21] M.J. Tahk, C.S. Park, C.K. Ryoo, Line-of-sight guidance laws for formation flight, Journal of Guidance, Control, and Dynamics 28 (4) (July–August 2005).

[22] G. Vachtsevanos, L. Tang, J. Reimann, An intelligent approach to coordinated control of multiple unmanned aerial vehicles, Presented at the American Helicopter Society 60th Annual Forum, Baltimore, MD, June 2004.

[23] A. Verma, C.N. Wu, V. Castelli, Autonomous command and control system for UAV formation, in: AIAA Atmospheric Flight Mechanics Conference and Exhibit, Austin, Texas, August 2003.

[24] S. Wan, G. Campa, M.R. Napolitano, B. Seanor, Y. Gu, Design of formation control laws for research aircraft models, AIAA 2003-5730, August 2003.